The Journal of Neuroscience, October 1, 1998, *18*(19):7891–7902

Promyelinating Schwann Cells Express Tst-1/SCIP/Oct-6

Edgardo J. Arroyo,[1] John R. Bermingham Jr,[2] Michael G. Rosenfeld,[2] and Steven S. Scherer[3]

Departments of [1]Neuroscience and [3]Neurology, The University of Pennsylvania Medical Center, Philadelphia, Pennsylvania 19104-6077, and [2]Howard Hughes Medical Institute, Department of Medicine, University of California, San Diego, La Jolla, California 92093-0623

Tst-1/SCIP/Oct-6, a POU domain transcription factor, is transiently expressed by developing Schwann cells and is required for their normal development into a myelinating phenotype. In *tst-1/scip/oct-6*–null sciatic nerves, Schwann cells are transiently arrested at the "promyelinating" stage, when they have a one-to-one relationship with an axon but before they have elaborated a myelin sheath. To determine when Schwann cells express Tst-1/SCIP/Oct-6, we examined β-galactosidase (β-gal) expression in heterozygous *tst-1/scip/oct-6* mice, in which one copy of the *tst-1/scip/oct-6* gene has been replaced with the LacZ gene. β-Gal expression from the LacZ gene seems to parallel Tst-1/SCIP/Oct-6 expression from the endogenous *tst-1/scip/oct-6* gene in developing and regenerating sciatic nerves. Furthermore, electron microscopic examination of 5-bromo-4-chloro-3-indolyl-β-D-galactopyranoside– (X-gal) and halogenated indolyl-β-D-galactoside– (Bluo-gal) stained nerves showed that promyelinating Schwann cells express the highest levels of β-gal, both in developing and in regenerating nerves. Thus, the expression of β-gal, a surrogate marker of Tst-1/SCIP/Oct-6, peaks at the same stage of Schwann cell development at which development is arrested in *tst-1/scip/oct-6*–null mice, indicating that Tst-1/SCIP/Oct-6 has a critical role in promyelinating Schwann cells.

Key words: myelin; transcription factors; cAMP; POU; axon–Schwann cell interactions; peripheral nerve; neuropathy

Schwann cells are the principal glial cell type in the PNS, and their development in rodents has been well described (Webster, 1993; Mirsky and Jessen, 1996; Zorick and Lemke, 1996). They originate from a subpopulation of neural crest cells that invade peripheral nerves at approximately embryonic day 13 (E13). These Schwann cell precursors do not have a basal lamina and require different growth factors than do immature Schwann cells, which first appear at E15–E16. Immature Schwann cell have a basal lamina, and their processes separate axons into small bundles. Cells with this morphological appearance persist until approximately postnatal day 20 (P20), and after this time they segregate small, unmyelinated axons into separate troughs and are called nonmyelinating Schwann cells. Myelinating Schwann cells are believed to arise from the same population of immature Schwann cells, differentiating in response to as yet undetermined axonal signal(s). The first morphological manifestation of a myelinating phenotype is a Schwann cell forming a one-to-one association with an axon, the so-called promyelinating Schwann cell, which then forms a myelin sheath within a few days. The onset of myelination is temporally dispersed, because the myelinated axons with the longest internodes and thickest myelin sheaths are myelinated first and those with the shortest internodes and thinnest sheaths are myelinated last (Hahn et al., 1987). By P30, the onset of myelination is complete, and all Schwann cells have one of two phenotypes: myelinating or nonmyelinating.

These morphological changes are accompanied by changes in gene expression (Mirsky and Jessen, 1996; Scherer and Salzer, 1996). Immature and nonmyelinating Schwann cells have a similar phenotype; both express neural cell adhesion molecule (N-CAM), L1, the low-affinity neurotrophin receptor/p75 ($p75^{NTR}$), growth-associated protein of 43 kDa (GAP-43), and glial fibrillary acidic protein. Myelinating Schwann cells, on the other hand, do not express these proteins but express a set of proteins that are components of the myelin sheath, such as protein zero (P_0), peripheral myelin protein of 22 kDa, myelin basic protein, connexin32, myelin-associated glycoprotein (MAG), and periaxin. The expression of these myelin-related proteins and their cognate mRNAs increases substantially as Schwann cells form myelin sheaths (Stahl et al., 1990; Lee et al., 1997), and this upregulation requires continuous axon–Schwann cell interactions both in developing and in regenerating nerves (Gupta et al., 1993; Scherer et al., 1994). Thus, the maintenance of the myelinating phenotype depends on axonal interactions, and there is emerging evidence that the various phenotypes of Schwann cells are related to the expression of different sets of transcription factors (Blanchard et al., 1996; Topilko et al., 1996; Zorick and Lemke, 1996; Scherer, 1997b).

Two unrelated transcription factors, Tst-1/SCIP/Oct-6 and Krox-20, are required for the normal development of myelinating Schwann cells, because their development is either transiently or permanently arrested at the promyelinating stage in *tst-1/scip/oct-6*– and *krox-20*–null mice, respectively (Topilko et al., 1994; Bermingham et al., 1996; Jaegle et al., 1996). The "arrested" promyelinating Schwann cells appear normal; they have a basal lamina, express MAG and periaxin, but do not form a myelin sheath. In spite of the similar phenotype of *tst-1/scip/oct-6*– and *krox-20*–null mice, these two transcription factors have a different

Received June 16, 1998; accepted July 10, 1998.

This work was supported by National Institutes of Health Grants NS34528 and NS37199 to S.S.S., by National Institute of General Medical Sciences Fellowship GM15020-04 to E.J.A., and by a grant from the National Multiple Sclerosis Society. We thank Susan Shumas and Yi-Tian Xu for technical assistance, Victor Ming for advice on statistical analysis, and Dr. Diane Sherman for immunoelectron microscopic analysis.

Correspondence should be addressed to Dr. Steven S. Scherer, 460 Stemmler Hall, 36th Street and Hamilton Walk, The University of Pennsylvania Medical Center, Philadelphia, PA 19104-6077.

temporal profile of expression; Tst-1/SCIP/Oct-6 mRNA is transiently expressed, peaking at approximately P1, whereas Krox-20 mRNA is expressed in parallel with other myelin-related genes, with high levels of expression even in adults (Monuki et al., 1989; Zorick et al., 1996). The expression of Tst-1/SCIP/Oct-6 in neonatal nerves and that of Krox-20 in adult nerves both depend on maintained axon–Schwann cell interactions, because their mRNA levels and immunoreactivity fall after axotomy (Scherer et al., 1994; Zorick et al., 1996). In this paper, we used the expression of the lacZ gene in heterozygous *tst-1/scip/oct-6* mice as a reporter for endogenous Tst-1/SCIP/Oct-6 expression. The product of the lacZ gene, β-galactosidase (β-gal), forms an electron-dense histochemical precipitate, allowing us to determine when Schwann cells express *tst-1/scip/oct-6*, both in developing and in lesioned sciatic nerves.

MATERIALS AND METHODS

tst-1/scip/oct-6 *heterozygous mice.* The creation and analysis of *tst-1/scip/oct-6* mice have been described (Bermingham et al., 1996). Heterozygous *tst-1/scip/oct-6* mice were maintained in a C57Bl/6 background at The University of Pennsylvania. All mice were genotyped by PCR (Bermingham et al., 1996).

Sciatic nerve crush and transection. Mice were anesthetized by intraperitoneal injection of 0.066 M 2,2,2-tribromoethanol diluted in 2-methyl-2-butanol (0.1 ml per 20 gm of body mass). Using aseptic technique, we exposed the sciatic nerves of adult anesthetized mice at the sciatic notch. Some nerves were doubly ligated and transected with fine scissors, and the two nerve stumps were sutured apart to prevent axonal regeneration. Nerve crush was produced by tightly compressing the sciatic nerve at the sciatic notch with flattened forceps twice, each time for 10 sec; this technique causes axonal degeneration but allows axonal regeneration. At varying times after nerve injury (8, 12, 24, and 58 d after the lesion), the animals were deeply anesthetized and processed for β-gal histochemistry or solution assay. Unlesioned nerves were collected from P1, P10, P30, and young adult (P60–P90) mice.

β-Gal solution assay. Nerves were frozen in liquid nitrogen, stored at −80°C, and then crushed with a steel mortar and pestle into a fine powder, mixed with lysis buffer in Eppendorf tubes (0.1 M potassium phosphate, pH 7.8, 0.2% Triton X-100, 0.5 mM dithiothreitol, and 0.2 mM PMSF), and sonicated on ice five times for 10 sec each. After a 30 min centrifugation, the supernatant was incubated for 60 min at 48°C to reduce the background level of β-gal activity. The amount of protein present in each sample was measured using the Bio-Rad (Hercules, CA) DC protein assay, and equal amounts of protein were assayed in triplicate for β-gal activity with the Galacton Light-Plus kit (Tropix) according to the manufacturer's instructions. For each sample, the protein concentration was diluted with lysis buffer to obtain a similar final concentration of protein (0.61 μg/μl for development and 0.49 μg/μl for nerve injury). Ten microliters of each sample were placed in a luminometer cuvette, mixed with an additional 10 μl of lysis buffer, and then mixed with 200 μl of reaction buffer [0.1 M phosphate buffer (PB), pH 8.0, and 1 mM MgCl]. After 15–30 min, 300 μl of Light Emission Accelerator reagent was added, and the cuvettes were placed in a luminometer. After allowing 10 sec for equilibration, the relative light units (RLU) were recorded in triplicate samples. For each experiment, a standard curve of RLU was constructed using purified β-gal (Sigma, St. Louis, MO).

5-Bromo-4-chloro-3-indolyl-β-D-galactopyranoside and halogenated indolyl-β-D-galactoside histochemistry. Anesthetized mice were perfused with 0.9% NaCl and then with 0.5% glutaraldehyde in 0.1 M PB, pH 7.4. In unlesioned animals, a piece of sciatic nerve, centered on the sciatic notch, was removed. In lesioned animals, the distal nerve stump was removed from the site of transection or crush to the popliteal fossa. To avoid the site of the lesion, we removed ~5 mm of the proximal end (nearest the site of the lesion) from crushed nerves; we removed 1–2 mm from transected nerves. The nerves were fixed for 1 hr in 0.5% glutaraldehyde in 0.1 M PB, rinsed in 0.1 M PB plus 2 mM $MgCl_2$, and then incubated overnight at 37°C in either 5-bromo-4-chloro-3-indolyl-β-D-galactopyranoside (X-gal) staining solution [35 mM $K_3Fe(CN)_6$, 35 mM $K_3Fe(CN)_6 \cdot {}^3H_2O$, 0.02% NP-40, 0.01% sodium deoxycholate, 2 mM $MgCl_2$, 0.1 M[R PB, AND 1 MG/ML X-GAL] OR HALOGENATED INDOLYL-B-[SCAP]D-galactoside (Bluo-gal) staining solution [3.1 mM $K_3Fe(CN)_6$, 3.1 mM $K_4Fe(CN)_6 \cdot {}^3H_2O$, 1 mM $MgCl_2$, 0.1 M PB, and 0.4 mg/ml Bluo-gal].

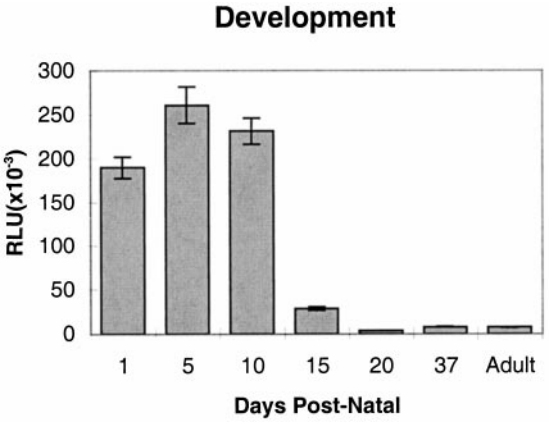

Figure 1. Solution assay of β-gal in developing *tst-1/scip/oct-6* +/− sciatic nerves. The *heights* of the *bars* represent the mean RLUs per milligram of protein for P1, P5, P10, P15, P20, P37, and adult mouse sciatic nerves. The RLUs were measured in triplicate for each sample; error bars represent the SEM.

The nerves were rinsed three times with 0.1 M PB, fixed in 3.6% glutaraldehyde (in 0.1 M PB) for 24 hr, rinsed twice in 0.1 M PB, osmicated, dehydrated in graded ethanols, and rapidly infiltrated in propylene oxide and epoxy to minimize the solubilization of X-gal and Bluo-gal. Semithin (500 nm) and thin (75 nm) transverse sections were cut from the sciatic notch region of unlesioned nerves and from the proximal end of the distal nerve stump from lesioned nerves. Sections were mounted on 200 mesh grids, stained with uranyl acetate and lead citrate, and examined with a Zeiss EM10 electron microscope. For every sample of nerve, a single section was selected for analysis. All cells with a complete nucleus (not obscured by grid bars) in the plane of the section were photographed at 8000–25,000× and were analyzed on the resulting prints according to their relationships with axons and the presence or absence of X-gal or Bluo-gal crystals. To demonstrate the crystals more clearly, we took the photographs (see Figs. 3, 4, 6) from sections that were not counterstained with lead citrate and uranyl acetate.

We performed a statistical analysis on the number of X-gal or Bluo-gal crystals in different kinds of Schwann cells in developing and regenerating nerves. Because the X-gal and Bluo-gal histochemistry cannot be assumed to be uniform between different nerves, all comparisons were made within the same sample of nerve. Crystals appeared to be rectangular in shape, but not preferentially oriented with respect to the nerve fibers, and were typically found at least in part within membranes. To count crystals, we examined the electron micrographs of individual Schwann cells in which the nucleus was in the plane of sections, and we considered an uninterrupted electron dense structure to be a single crystal. In developing nerves, we compared the number of crystals in bundling, in promyelinating, and in myelinating Schwann cells by the Wilcoxon rank-sum test (JMP IN) (Hollander and Wolfe, 1973); in regenerating nerves, we compared the number of crystals in promyelinating; in myelinating; in bundling, promyelinating > 1, and nonmyelinating; and in perineurial-like cells.

RESULTS

The developmental expression of β-gal parallels that of endogenous Tst-1/SCIP/Oct-6 protein

Because the lacZ gene essentially replaced the *tst-1/scip/oct-6* gene without disrupting its promoter (Bermingham et al., 1996), the level of β-gal protein in heterozygous *tst-1/scip/oct-6* (*tst-1/scip/oct-6* +/−) nerves should parallel the expression of the Tst-1/SCIP/Oct-6 protein itself. To determine this directly, we analyzed *tst-1/scip/oct-6* +/− sciatic nerves from mice of different ages with a sensitive, luminometric assay of β-gal. Figure 1 shows the result of one set of assays. The RLU was high at P1, peaked at P5, and rapidly diminished after P10, so that by P20 the levels were comparable with that in adults. We repeated this assay using a different set of *tst-1/scip/oct-6* +/− sciatic nerves and found

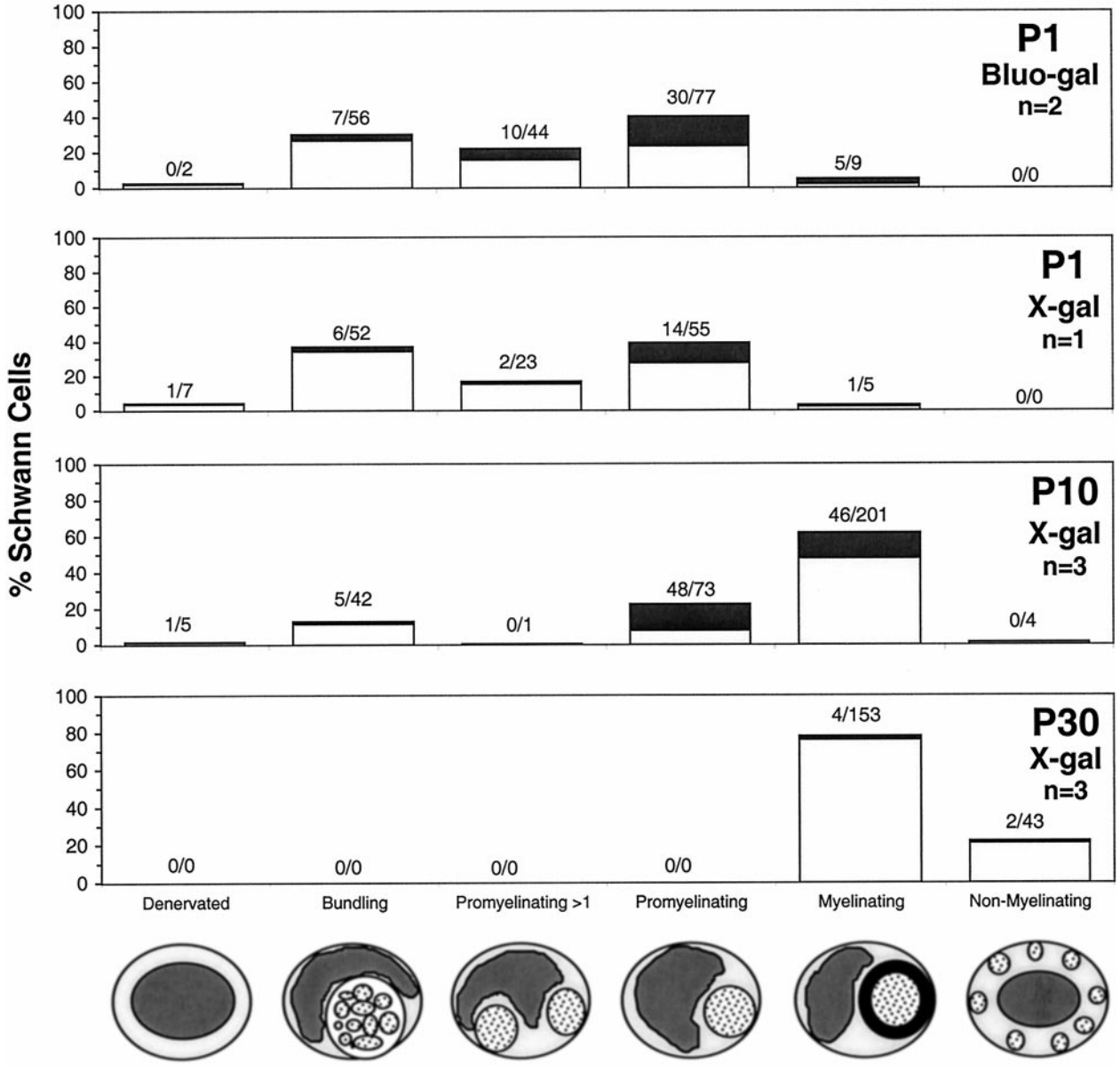

Figure 2. Graphical summary of β-gal expression in Schwann cells in *tst-1/scip/oct-6* +/− sciatic nerves. At each developmental age (P1, P10, and P30), the *heights* of the *bars* show the percentage of Schwann cells of the following morphologies: denervated, bundling, promyelinating > 1, promyelinating, myelinating, and nonmyelinating. The *lightly shaded portions* of the *bars* indicate the percentage of β-gal–negative cells, whereas the *darkly shaded portions* represent the percentage of β-gal–positive Schwann cells (visualized with X-gal and Bluo-gal at P1 and with X-gal at P10 and P30). The fraction *over* each *bar* shows the number of positive Schwann cells relative to the total number of Schwann cells of that morphology. *n*, Number of nerves analyzed at each age.

similar results (data not shown). The RLUs of sciatic nerves from age-matched wild-type littermates, in contrast, were low at every age tested, ranging from ~1500 to ~4000, always less than the lowest values found in *tst-1/scip/oct-6* +/− mice at any age. Thus, the overall pattern of β-gal expression in developing *tst-1/scip/oct-6* +/− nerves matches that of Tst-1/SCIP/Oct-6 mRNA in developing rat sciatic nerves (Monuki et al., 1989; Scherer et al., 1994; Zorick et al., 1996).

tst-1/scip/oct-6 +/− promyelinating Schwann cells express β-gal

The above data justify using β-gal expression as a surrogate marker of the endogenous *tst-1/scip/oct-6* gene expression. Because myelination appears normal in *tst-1/scip/oct-6* +/− mice (Bermingham et al., 1996; Jaegle et al., 1996), we examined *tst-1/scip/oct-6* +/− nerves after staining them with X-gal or Bluo-gal. In the presence of β-gal, these sugars produce a blue precipitate that becomes electron dense after osmication. We examined sciatic nerves from P1, P10, and P30 *tst-1/scip/oct-6* +/− mice, a range of ages that encompasses the onset of myelination and the peak of Tst-1/SCIP/Oct-6 expression. P1 and P10 nerves were grossly blue, but P30 nerves were only lightly stained, in agreement with the luminometric β-gal assays, demonstrating again that β-gal expression falls during postnatal development.

To determine precisely which Schwann cells express β-gal, we performed electron microscopy on these sciatic nerves, because this allowed axon–Schwann cell relationships to be more accu-

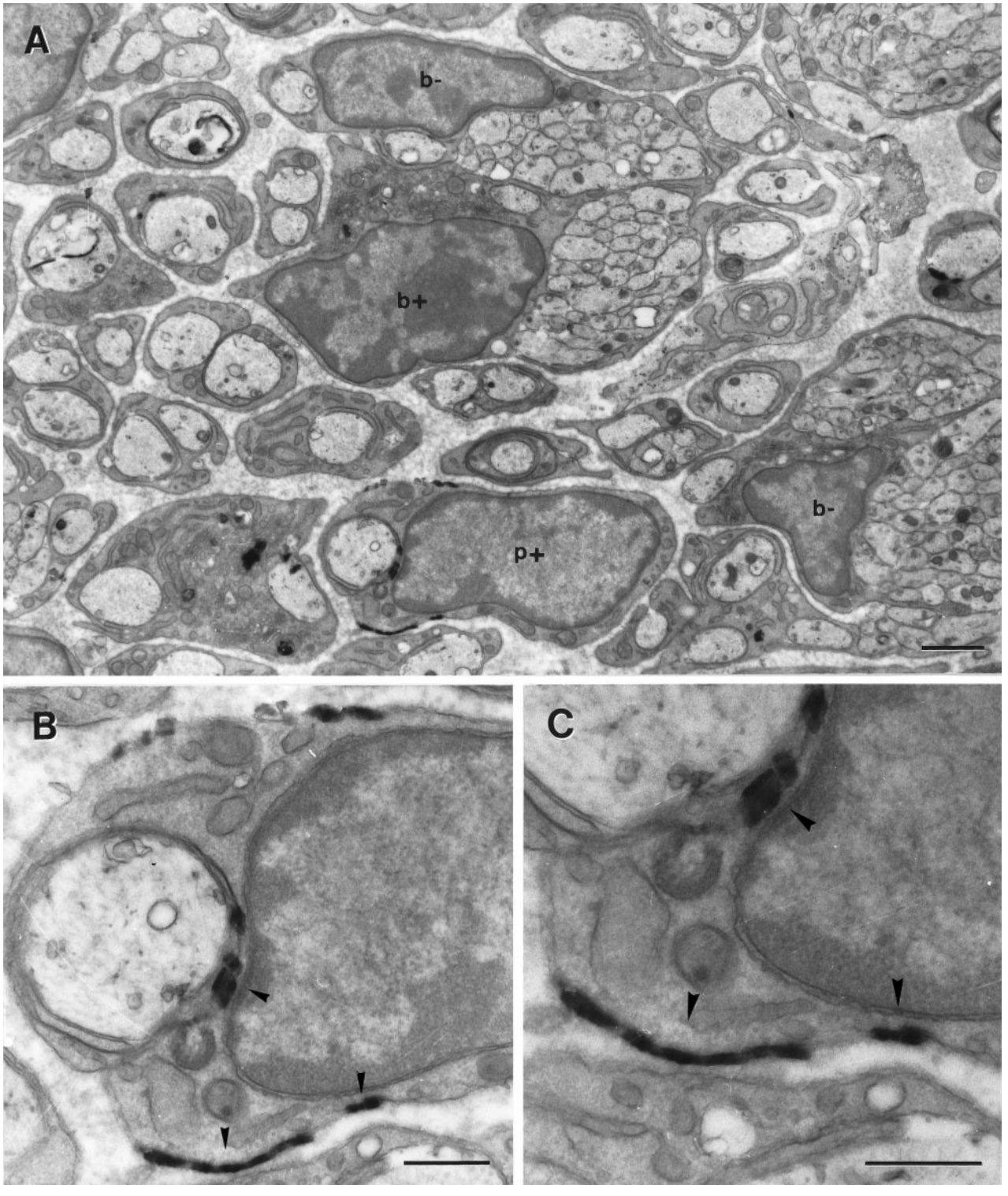

Figure 3. Electron microscopy of P1 *tst-1/scip/oct-6* +/− sciatic nerve stained with Bluo-gal. *A*, The nuclei of three bundling (*b*) Schwann cells and one promyelinating (*p*) Schwann cell. *B*, *C*, Higher magnifications of the promyelinating Schwann cell seen in *A*. Some of the Bluo-gal crystals are indicated (*arrowheads*); the *symbols plus* and *minus* mark the presence or absence, respectively, of crystals in classified cells. To demonstrate the crystals more clearly, we took these photographs from a section that was not counterstained with lead citrate and uranyl acetate. Scale bars: *A*, 1.0 μm; *B*, *C*, 0.5 μm.

rately determined than can be done by light microscopy. Every nucleated Schwann cell that was visible in a single transverse section was photographed and classified by its morphological relationship to axons (Webster, 1993), and the presence or absence of X-gal or Bluo-gal crystals was noted. As shown schematically in Figure 2, we classified Schwann cells as follows: denervated (not associated with any axon), bundling (associated with more than one axon, typically many axons, but not individually ensheathing any of them), promyelinating (ensheathing one axon), promyelinating more than one axon (promyelinating > 1;

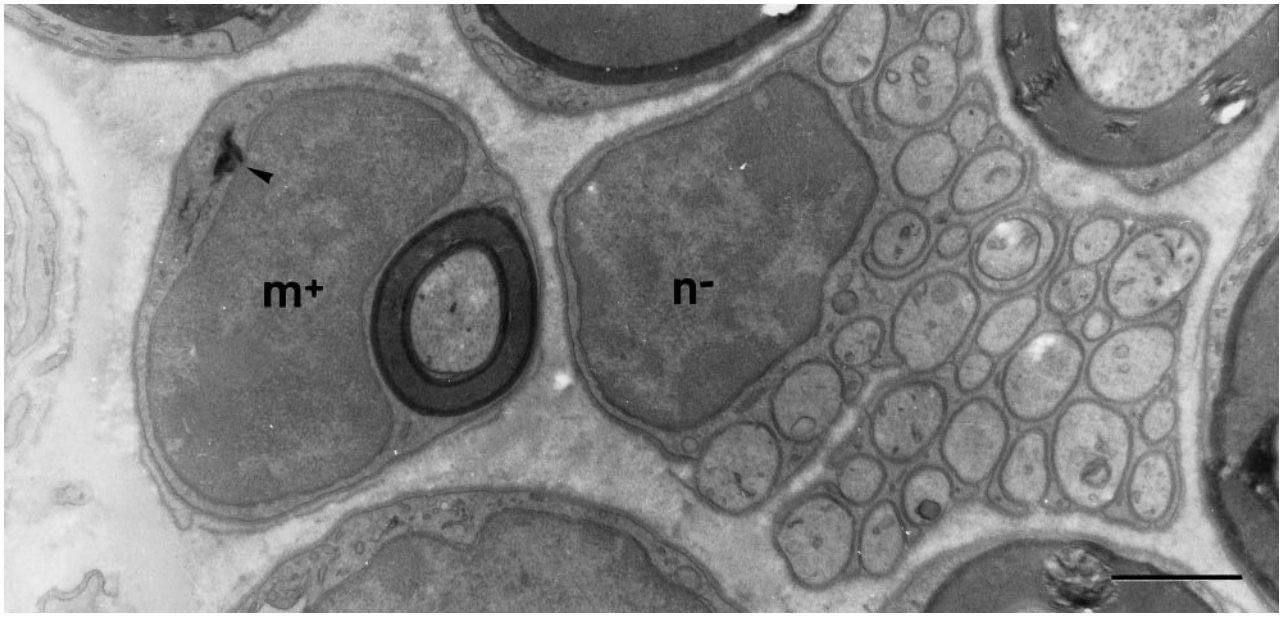

Figure 4. Electron microscopy of P30 *tst-1/scip/oct-6* +/− sciatic nerve stained with Bluo-gal. Two Schwann cells, one myelinating (*m*) and one nonmyelinating (*n*), are shown. The *arrowhead* indicates a Bluo-crystal. The *symbols plus* and *minus* mark the presence or absence, respectively, of crystals in classified cells. To demonstrate the crystals more clearly, we took these photographs from a section that was not counterstained with lead citrate and uranyl acetate. Scale bar, 1.0 μm.

individually ensheathing more than one axon), myelinating (wrapping an individual axon more than once or forming compact myelin), or nonmyelinating (ensheathing more than one axon). At P1 and P10, we classified Schwann cells that were associated with nonmyelinated axons as either bundling or promyelinating, whereas at P30, all of these were considered to be nonmyelinating Schwann cells according to morphological criteria (Peters and Muir, 1959; Kobayashi and Suzuki, 1990; Webster, 1993).

In P1 *tst-1/scip/oct-6* +/− or *tst-1/scip/oct-6* +/+ nerves, most Schwann cells were bundling and promyelinating, as reported by Bermingham et al. (1996). Light microscopic examination of X-gal–treated nerves, however, revealed that blue crystals were only seen in *tst-1/scip/oct-6* +/− nerves, mainly in what appeared to be promyelinating Schwann cells. By the use of electron microscopy, the X-gal crystals were electron dense and concentrated in the nuclear membrane (Feltri et al., 1992). Most X-gal–positive cells were promyelinating Schwann cells, although some bundling and myelinating Schwann cells were also positive (Fig. 2). In addition to Schwann cells, there was a small population of fibroblasts and macrophages; these cells were X-gal–negative (data not shown). In addition to X-gal, we also used Bluo-gal to produce bigger and more conspicuous crystals, which were also found in other membranous components of the cell, especially the plasma membrane (Fig. 3). Although Bluo-gal appeared to be more sensitive than X-gal, staining a higher proportion of promyelinating and myelinating Schwann cells, the results were essentially the same (Fig. 2).

In P10 *tst-1/scip/oct-6* +/− and *tst-1/scip/oct-6* +/+ nerves, the number of myelinating Schwann cells increased substantially compared with that in P1 nerves (Fig. 2). In *tst-1/scip/oct-6* +/− nerves, a high proportion of myelinating and promyelinating Schwann cells had X-gal crystals, especially the latter. As in P1 nerves, fibroblasts and macrophages did not have X-gal crystals, and Schwann cells in *tst-1/scip/oct-6* +/+ nerves did not have X-gal crystals.

Table 1. Quantitative analysis of X-gal or Bluo-gal expression in individual Schwann cells of P1 and P10 *tst-1/scip/oct-6* ± sciatic nerves

	N	Range	Mean ± SEM	*P*>
P1 nerve Bluo-gal				
Nerve 1				
Bundling	20	0–6	0.55 ± 0.32	0.11
Promyelinating	51	0–12	1.5 ± 0.38	
Nerve 2				
Bundling	40	0–4	0.25 ± 0.14	0.0001
Promyelinating	29	0–9	1.9 ± 0.50	
P1 nerve X-gal				
Bundling	51	0–2	0.10 ± 0.05	0.003
Promyelinating	54	0–6	0.87 ± 0.22	
P10 nerve X-gal				
Nerve 1				
Bundling	7	0	0 ± 0	0.006
Promyelinating	16	0–8	2.7 ± 0.63	
Myelinating	12	0–3	0.25 ± 0.09	0.0001
Nerve 2				
Bundling	14	0–2	0.14 ± 0.14	0.0002
Promyelinating	29	0–6	2.2 ± 0.37	
Myelinating	50	0–6	1.2 ± 0.24	0.02
Nerve 3				
Bundling	20	0–1	0.15 ± 0.08	0.004
Promyelinating	33	0–5	1.1 ± 0.24	
Myelinating	104	0–4	0.23 ± 0.07	0.0001

Schwann cells were classified as bundling, promyelinating, or myelinating. For each kind of Schwann cell in each nerve, the number of Schwann cells counted (*N*), the range, and the mean (±SEM) number of crystals are indicated. The numbers of crystals in promyelinating Schwann cells were compared to that in bundling or myelinating Schwann cells by the Wilcoxon rank-sum test (*P*, probability).

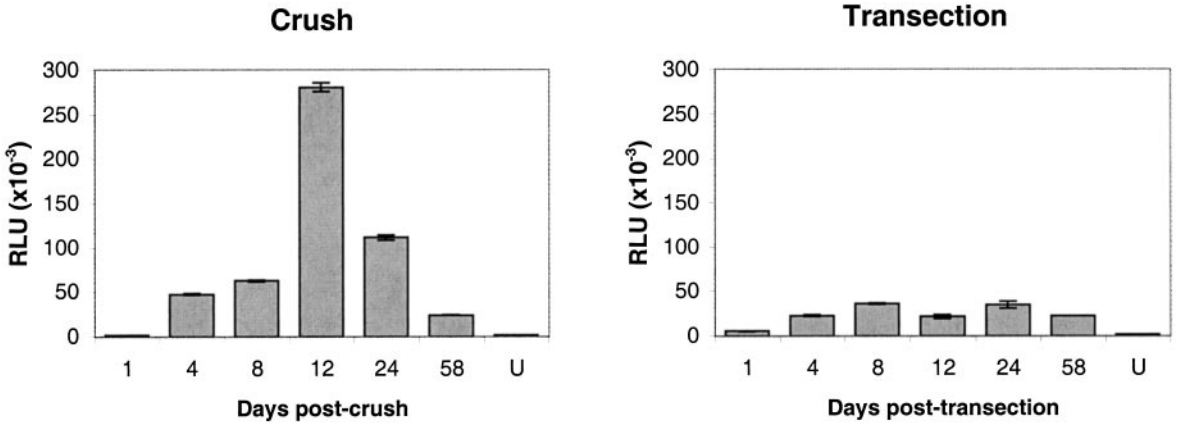

Figure 5. Solution assay of β-gal in adult *tst-1/scip/oct-6* +/− sciatic nerves. The *heights* of the *bars* represent the mean RLUs per milligram of protein from the distal stumps of nerves 1, 4, 8, 12, 24, and 58 d after transection or after crushing. Note that the RLUs of the crushed nerves is higher than that in the transected nerves during the period of ensheathment and myelination (8–24 d after crushing).

Figure 6. Electron micrograph of a perineurial-like cell from the distal stump 24 d after crushing. This cell shows the typical features, including a patchy basal lamina (*fat arrows*), caveoli (*arrowheads*), and two long processes that ensheathe Schwann cells (*s*) and axons (*a*). Scale bar, 1.0 μm.

P30 *tst-1/scip/oct-6* +/− and *tst-1/scip/oct-6* +/+ nerves contained only myelinating and nonmyelinating Schwann cells (Figs. 2, 4). In addition to the occasional X-gal– or Bluo-gal–positive Schwann cell (Figs. 2, 4), we did not note any differences between *tst-1/scip/oct-6* +/− and *tst-1/scip/oct-6* +/+ nerves (Bermingham et al., 1996; Jaegle et al., 1996).

The above results, taken together, demonstrate a dynamic, maturation-dependent expression of β-gal in *tst-1/scip/oct-6* +/− Schwann cells. The proportion of cells expressing β-gal indicates that some bundling Schwann cells express low levels of β-gal but that β-gal expression increases dramatically in promyelinating Schwann cells and then decreases after the onset of myelination. To analyze further the stage-specific expression of β-gal, we counted the number of X-gal or Bluo-gal crystals in Schwann cells of P1 and P10 *tst-1/scip/oct-6* +/− nerves. Because the degree of staining of individual nerves with X-gal or Bluo-gal histochemistry cannot be assumed to be the same, comparisons were made within individual nerves. These results are summarized in Table 1. In P1 nerves, there were more crystals in promyelinating Schwann cells than in bundling Schwann cells; the number of myelinating Schwann cells was too low to analyze. In P10 nerves, there were more crystals in promyelinating Schwann cells than in either bundling or myelinating Schwann cells. Thus, promyelinating Schwann cells had both the highest proportion and the highest number of X-gal or Bluo-gal crystals, indicating that these cells express the highest levels of β-gal and, by inference, Tst-1/SCIP/Oct-6.

β-gal expression in lesioned adult nerves

Lesioning adult nerves disrupts axon–Schwann cell interactions and leads to the dedifferentiation of Schwann cells, most pronounced in myelinating Schwann cells, which cease expressing

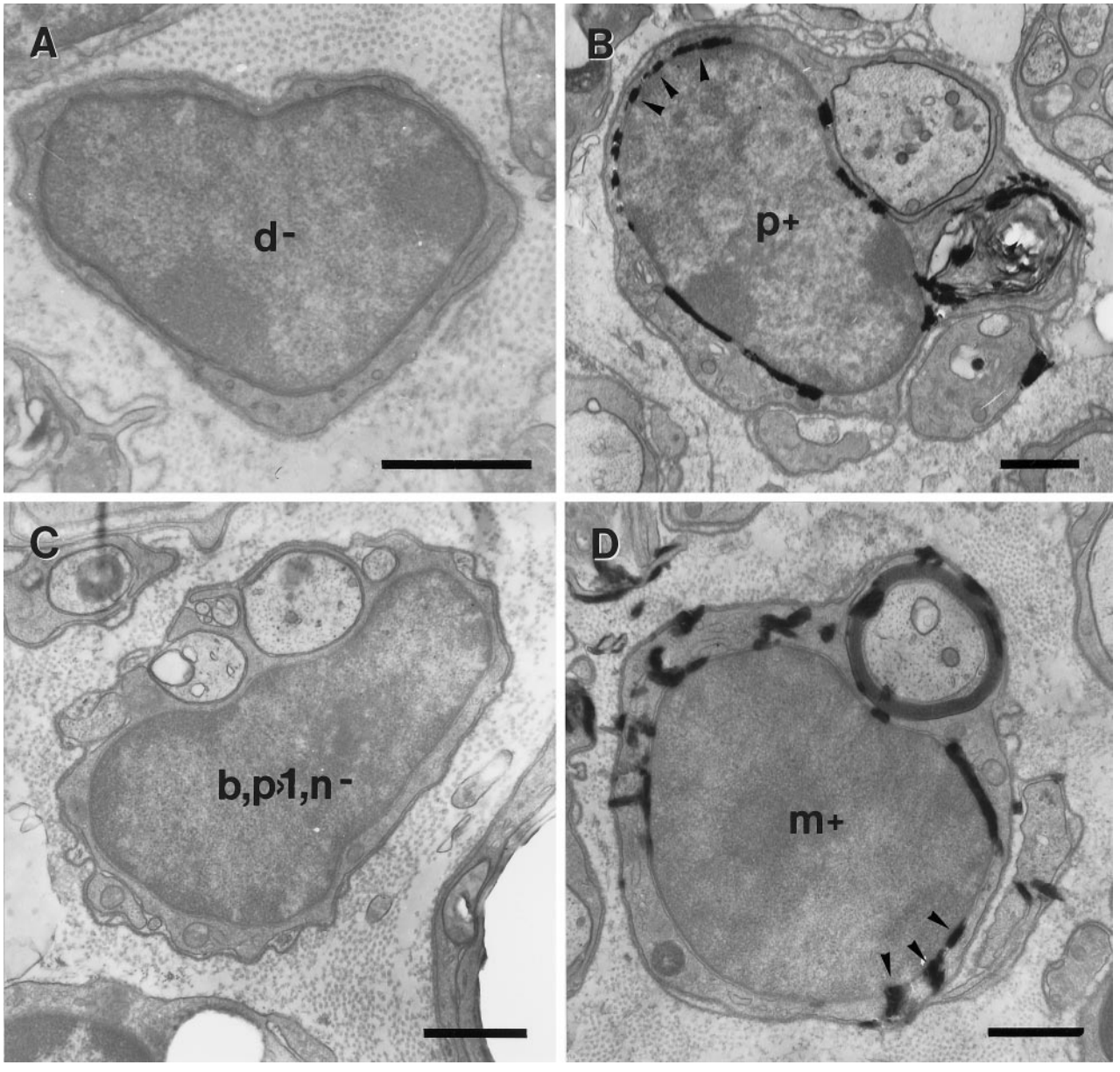

Figure 7. Electron microscopy of lesioned adult *tst-1/scip/oct-6* +/− sciatic nerves stained with Bluo-gal. *A*, A denervated (*d*) Schwann cell at 12 d after transection. *B–D*, Promyelinating (*p*); bundling, promyelinating > 1, and nonmyelinating (*b*,*p*>1,*n*); and myelinating (*m*) Schwann cells at 12 d after crushing, respectively. Some Bluo-gal crystals are indicated (*arrowheads*). The *symbols plus* and *minus* indicate the presence or absence, respectively, of crystals in classified cells. To demonstrate the crystals more clearly, we took these photographs from sections that were not counterstained with lead citrate and uranyl acetate. Scale bars, 1.0 μm.

myelin-related genes and begin expressing markers typical of immature Schwann cells, such as N-CAM, L1, $p75^{NTR}$, and GAP-43 (Mirsky and Jessen, 1996; Scherer, 1997b). In permanently transected nerves, in which axons are deliberately prevented from regenerating, Schwann cells remain dedifferentiated indefinitely. In crushed nerves, axons readily regenerate, and some are remyelinated by Schwann cells, whose differentiation appears to recapitulate that seen in development, including the re-expression of Tst-1/SCIP/Oct-6 mRNA and protein (Scherer et al., 1994; Zorick et al., 1996).

To confirm and extend these findings, we performed β-gal assays on crushed and permanently transected sciatic nerves from adult *tst-1/scip/oct-6* +/− and *tst-1/scip/oct-6* +/+ mice. We analyzed the amount of β-gal activity in nerve segments distal to the site of injury at 1, 4, 8, 12, 24, and 58 d after crushing and after transection (Fig. 5). In *tst-1/scip/oct-6* +/− mice, the amount of β-gal activity in the distal nerve stumps of crushed nerves increased substantially between 1 and 12 d, followed by a decline. The amount of β-gal activity in the distal nerve stumps of transected nerves, in contrast, increased only slightly over this same time frame. The higher levels of β-gal activity in crushed nerves coincide with the re-ensheathment and remyelination of regenerating axons and, overall, agree with the previous studies of Tst-1/SCIP/Oct-6 expression in lesioned adult rat sciatic nerves (Monuki et al., 1990; Scherer et al., 1994; Zorick et al., 1996). The β-gal activity in both transected and crushed adult *tst-1/scip/oct-6* +/+ nerves was low, comparable with that in unlesioned adult *tst-1/scip/oct-6* +/− nerves (data not shown), further demonstrat-

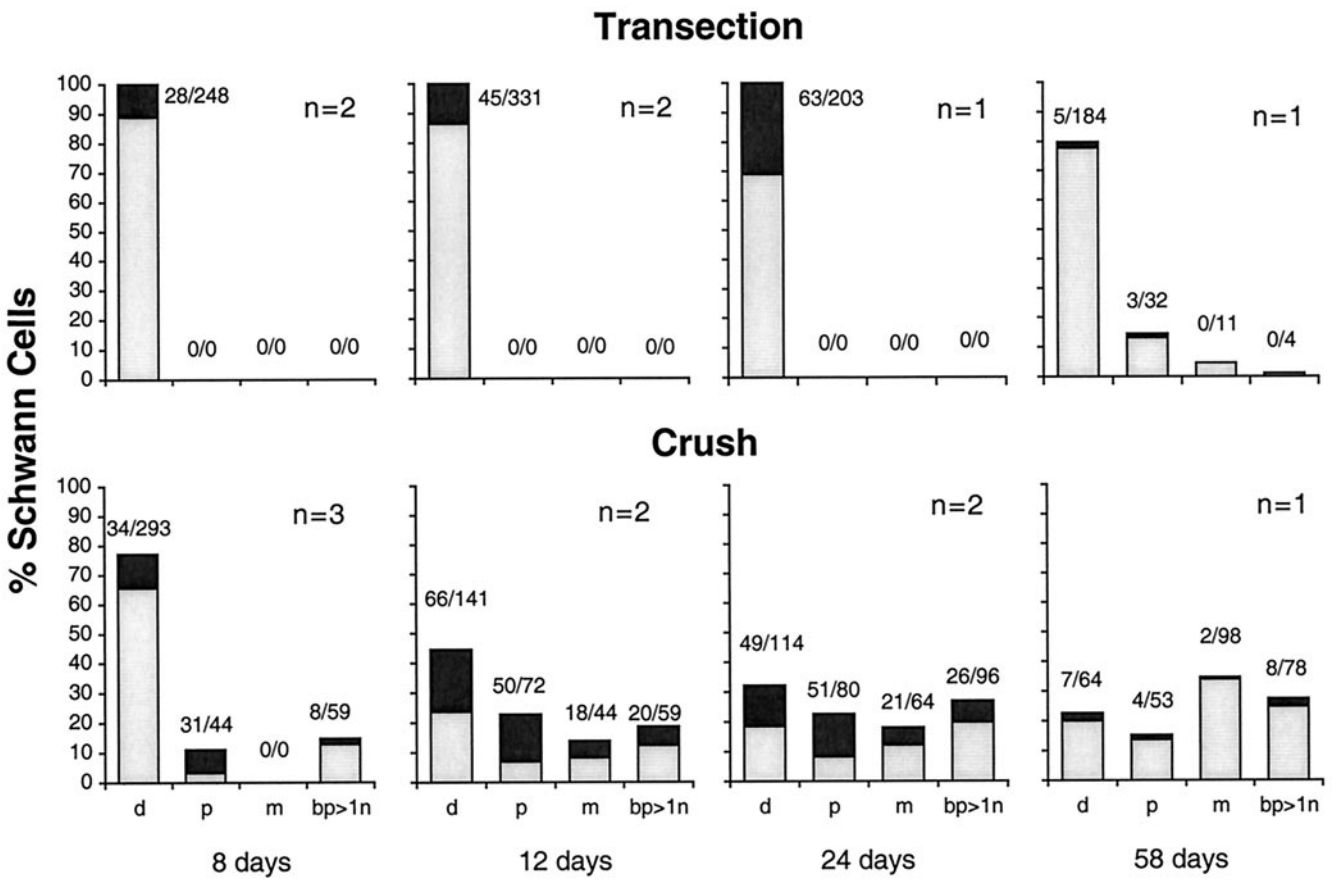

Figure 8. Graphical summary of β-gal expression by Schwann cells in lesioned adult *tst-1/scip/oct-6* +/− sciatic nerves. The *bars* show the percentage of Schwann cells of each morphology at 8, 12, 24, and 58 d after transection (*upper*) and after crushing (*lower*); the *lightly* and *darkly shaded bars* indicate the percentage of Bluo-gal–negative and –positive Schwann cells, respectively. The fraction *over* each *bar* shows the number of positive Schwann cells relative to the total number of Schwann cells of that morphology. *n*, Number of animals analyzed. The Schwann cell morphologies are as follows: *d*, denervated; *bp*>1*n*, bundling, and promyelinating > 1, and nonmyelinating; *p*, promyelinating; and *m*, myelinating.

ing that the increase in transected and crushed *tst-1/scip/oct-6* +/− nerves is not the result of nerve-injury per se but rather is the result of increased Tst-1/SCIP/Oct-6 expression.

Promyelinating and denervated Schwann cells express β-gal in lesioned nerves

To determine which Schwann cells express Tst-1/SCIP/Oct-6 in lesioned adult *tst-1/scip/oct-6* +/− nerves, we examined the distal nerve stumps of lesioned nerves (8, 12, 24, and 58 d after the lesion) by electron microscopy after Bluo-gal histochemistry. At 8 d after transection, there were a few axonal remnants, and all of the myelin sheaths were degenerating. Between 8 and 58 d after transection, the amount of myelin debris progressively diminished, and it was increasing found in macrophages rather than in Schwann cells. Thus, by 58 d after transection, denervated Schwann cells and macrophages were the predominant cell types in lesioned nerves. At 24 and 58 d, lesioned nerves also contained perineurial-like cells, which typically had a discontinuous basal lamina, caveoli, and elongated processes that often partially surrounded Schwann cells (Fig. 6); these looked different than denervated Schwann cells, which were primarily oval in shape and surrounded by a complete basal lamina (Fig. 7*A*). These perineurial-like cells have been noted previously in lesioned nerves, but their cellular origin (Schwann cell vs endoneurial fibroblast) has not been resolved (Morris et al., 1972). Even though nerves had been deliberately transected to prevent axonal regeneration, at 58 d there were a few axons that had regenerated (Fig. 8); these were associated with Schwann cells.

In crushed adult *tst-1/scip/oct-6* +/− nerves, axons and myelin sheaths degenerated in a similar manner to that in transected nerves, but axonal regeneration occurred. At 8 d, most Schwann cells were denervated, but some were associated with bundles of regenerating axons or with single regenerating axons in a one-to-one promyelinating configuration. At 12 and 24 d, a higher proportion of Schwann cells was associated with regenerating axons, which were more numerous than at 8 d, and some Schwann cells had myelinated regenerating axons (Fig. 7*B–D*). By 58 d, nerves had assumed a more mature appearance, with more myelinating and nonmyelinating Schwann cells and fewer denervated and bundling Schwann cells than at 24 d. Thus, the morphological aspects of axon–Schwann cell interactions that culminate in myelination appear to be similar in developing and regenerating nerves.

To determine which cells expressed β-gal, we determined the proportion of cells with Bluo-gal crystals in a single, transverse section of lesioned adult *tst-1/scip/oct-6* +/− nerves. After transection, the proportion of denervated Schwann cells with Bluo-gal crystals varied between 3 and 31% (Fig. 8). Whether these different proportions at various times after transection represent significant differences, however, is moot, because the overall level of β-gal activity in the distal stumps of transected nerves in-

Table 2. Quantitative analysis of X-gal and Bluo-gal expression in individual Schwann cells from *tst-1/scip/oct-6* sciatic nerves 8, 12, and 24 days after crushing

	N	Range	Mean ± SEM	*P*>
8 D Bluo-gal				
Nerve 1				
Denervated	72	0–17	1.2 ± 0.37	0.0001
Promyelinating	19	0–29	8.4 ± 1.65	
$b/p > 1/n$	11	0–10	2.3 ± 1.21	0.009
Nerve 2				
Denervated	147	0–13	0.30 ± 0.12	0.0001
Promyelinating	7	0–7	4.7 ± 0.99	
$b/p > 1/n$	18	0–7	0.44 ± 0.39	0.0001
Nerve 3				
Denervated	89	0–5	0.27 ± 0.09	0.0001
Promyelinating	18	0–12	2.4 ± 0.85	
$b/p > 1/n$	30	0–8	0.73 ± 0.36	0.03
12 D Bluo-gal				
Nerve 1				
Denervated	50	0–15	1.9 ± 0.5	0.003
Promyelinating	53	0–24	4.5 ± 0.8	
Myelinating	36	0–15	1.8 ± 0.56	0.009
$b/p > 1/n$	39	0–17	2.3 ± 0.65	0.03
Nerve 2				
Denervated	91	0–19	2.4 ± 0.41	0.0001
Promyelinating	19	0–26	11 ± 1.9	
Myelinating	8	0–17	8 ± 2.38	0.42
$b/p > 1/n$	10	0–15	3.2 ± 1.6	0.004
12 D X-gal				
Denervated	120	0–5	0.3 ± 0.07	0.0001
Promyelinating	39	0–9	2.2 ± 0.50	
Myelinating	10	0–14	3.2 ± 1.44	0.46
$b/p > 1/n$	19	0–9	0.68 ± 0.49	0.03
24 D Bluo-gal				
Nerve 1				
Denervated	20	0–1	0.05 ± 0.05	0.30
Promyelinating	21	0–16	1.5 ± 0.9	
Myelinating	34	0–12	0.9 ± 0.43	0.94
$b/p > 1/n$	44	0–5	0.4 ± 0.17	0.79
Nerve 2				
Denervated	94	0–19	2.3 ± 0.33	0.0001
Promyelinating	59	0–21	6.2 ± 0.69	
Myelinating	30	0–13	3.2 ± 0.74	0.005
$b/p > 1/n$	52	0–20	2.0 ± 0.48	0.0001

Schwann cells were classified as denervated; promyelinating; bundling, promyelinating > 1, and nonmyelinating ($b/p > 1/n$); or myelinating; perineurial-like cells were also analyzed. For each kind of cell in each nerve, the number of cells counted (*N*), the range, and the mean (±SEM) number of crystals are indicated. The numbers of crystals in promyelinating Schwann cells were compared to that in denervated, $b/p > 1/n$, and myelinating Schwann cells by the Wilcoxon rank-sum test (*P*, probability).

creased only slightly after transection (Fig. 5). In addition to being found in Schwann cells, Bluo-gal crystals were also found in some macrophages and rarely in perineurial-like cells.

Because the axon–Schwann cell interactions that lead to myelination in regenerating nerves appear to recapitulate those in developing nerves, it seemed likely that promyelinating Schwann cells in crushed nerves would also have the highest levels of β-gal. To determine whether this was case, we examined the Schwann cells in the distal stumps of crushed adult *tst-1/scip/oct-6* +/− nerves for the presence of X-gal or Bluo-gal crystals. For this analysis, we lumped together bundling, promyelinating > 1, and nonmyelinating Schwann cells together into a single category ($b,p>1,n$) (Fig. 7*C*), because it is difficult to distinguish these potentially different kinds of Schwann cells in lesioned nerves and, particularly, because single Schwann cells may ensheathe misdirected axons from sensory, motor, and autonomic neurons (King and Thomas, 1971; Scherer and Easter, 1984). As summarized in Figure 8 and Table 2, a high proportion of promyelinating Schwann cells contained Bluo-gal crystals in crushed nerves, and promyelinating Schwann cells had significantly more Bluo-gal crystals than did denervated or $b,p>1,n$ Schwann cells at all time points. In some nerves, promyelinating Schwann cells had more crystals than did myelinating Schwann cells. Although the number of perineurial-like cells was variable, a low proportion of these cells also had Bluo-gal crystals. These data, taken together, show that the timing of higher β-gal activity in crushed nerves is related to the ensheathment and myelination of regenerating axons and not to Wallerian degeneration per se. During the peak of β-gal expression, at approximately 12 d after crushing, promyelinating and myelinating Schwann cells account for the bulk of β-gal expression and, hence, are the cells that express the highest levels of Tst-1/SCIP/Oct-6. In further support of these conclusions, we did not find crystals in the lesioned adult *tst-1/scip/oct-6* +/+ nerves at 12 d after transection and after crushing (data not shown).

DISCUSSION

In this paper, we demonstrate for the first time that Tst-1/SCIP/Oct-6 is principally expressed by promyelinating Schwann cells. Whereas the timing of Tst-1/SCIP/Oct-6 expression in developing and lesioned peripheral nerves was consistent with the idea that it functions in proliferating Schwann cells (Monuki et al., 1990), subsequent anatomical studies suggested that Tst-1/SCIP/Oct-6 expression may be independent of proliferation and that it functions in promyelinating Schwann cells (Scherer et al., 1994). The observation that Schwann cells are temporarily arrested at the promyelinating stage in *tst-1/scip/oct-6*–null mice is further evidence that it plays an essential role at these cells (Bermingham et al., 1996; Jaegle et al., 1996).

Does β-gal expression reflect Tst-1/SCIP/Oct-6 expression?

We used the expression of β-gal in *tst-1/scip/oct-6* +/− mice as a means of identifying when Schwann cells express Tst-1/SCIP/Oct-6. This analysis assumes that the expression of one copy of *tst-1/scip/oct-6* is sufficient for the normal development of myelinating Schwann cells. This assumption seems to be justified as *tst-1/scip/oct-6* +/− mice are long-lived and without a discernable phenotype (Bermingham et al., 1996; Jaegle et al., 1996), and we have not seen any difference in the degree of myelination between *tst-1/scip/oct-6* +/− and *tst-1/scip/oct-6* +/+ mice in several litters (S. S. Scherer and E. J. Arroyo, unpublished observations).

Our analysis also requires that the expression of *lacZ* mirrors that of *tst-1/scip/oct-6*. This is likely to be the case. First, the design of the targeting vector did not disrupt the *tst-1/scip/oct-6* promoter, because only the open reading frame was replaced by the expression cassette (which contained *lacZ* and *neo*), leaving the *tst-1/scip/oct-6* promoter intact (Bermingham et al., 1996). Furthermore, the theoretical possibility that promoter elements within *tst-1/scip/oct-6* may be disrupted by the homologous recombination of the targeting vector does not apply, because it is an intronless gene (Kuhn et al., 1991). Second, although the half-life

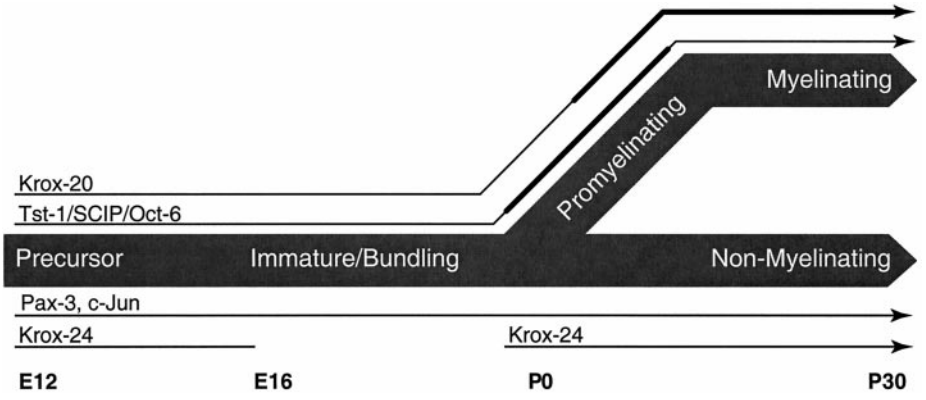

Figure 9. Schematic view of transcription factor expression in developing rodent Schwann cells. This figure summarizes the timing of expression of various transcription factors in developing rodent (mouse and rat) peripheral nerve and relates the expression of these transcription factors to the anatomical relationships of axons and Schwann cells. The *thick black lines* (e.g., for Krox-20 and Tst-1/SCIP/Oct-6) indicate relatively higher levels of expression than do the *thin black lines*.

of β-gal and Tst-1/SCIP/Oct-6 may be different, this should not affect our interpretation. The reported half-life of *E. coli* β-gal in mammalian cells varies from 13 to 43 hr (Margolis et al., 1993; Jacobsen and Willumsen, 1995); this is probably longer than the half-life of Tst-1/SCIP/Oct-6, because the expression of Tst-1/SCIP/Oct-6 protein decreases markedly in neonatal rat sciatic nerve by 1 d after axotomy (S. S. Scherer, unpublished observations). Even if β-gal were very stable, this should not significantly alter the onset of β-gal expression and, hence, our conclusion that Tst-1/SCIP/Oct-6 expression peaks in promyelinating Schwann cells. Stable β-gal would, however, prolong the fall of β-gal expression, so that we may have overestimated the duration of Tst-1/SCIP/Oct-6 expression by myelinating Schwann cells. Third, the pattern of β-gal expression in developing and injured peripheral nerves parallels the expression of Tst-1/SCIP/Oct-6 mRNA described in rats. In developing *tst-1/scip/oct-6* +/− sciatic nerve, our luminometric assays show an apparent peak of β-gal at P5. Although Tst-1/SCIP/Oct-6 protein levels have not been measured in mice or rats, the peak of Tst-1/SCIP/Oct-6 mRNA in rats occurs somewhat earlier (approximately P1) (Monuki et al., 1989, 1990; Scherer et al., 1994). The slight delay in β-gal expression compared with that of Tst-1/SCIP/Oct-6 mRNA may reflect the time required for protein synthesis and accumulation or a species differences.

Tst-1/SCIP/Oct-6 is mainly expressed by promyelinating Schwann cells

The above discussion justifies the use of the β-gal histochemistry as a means of identifying which Schwann cells express Tst-1/SCIP/Oct-6. Although one can detect Tst-1/SCIP/Oct-6 by immunohistochemistry, the phenotype of these cells is difficult to assess by light microscopy (Scherer et al., 1994; Blanchard et al., 1996; Zorick et al., 1996). The differentiated state of a Schwann cell can be established by electron microscopy, but our attempts to perform immunoelectron microscopy with the Tst-1/SCIP/Oct-6 antibody were unsuccessful (D. L. Sherman and S. S. Scherer, unpublished observations). β-Gal histochemistry, however, allowed us to determine that Tst-1/SCIP/Oct-6 is mainly expressed by promyelinating Schwann cells, both in developing and in regenerating nerves. Bundling Schwann cells express less β-gal, and myelinating Schwann cells appear to express β-gal only transiently. The peak of β-gal expression coincides with the promyelinating morphology, which is also the point at which Schwann cell development is transiently arrested in *tst-1/scip/oct-6*–null mice (Bermingham et al., 1996; Jaegle et al., 1996). The finding that not all promyelinating and myelinating Schwann cell have X-gal crystals, however, should not be interpreted as evidence that these cells do not express β-gal. Rather, this is probably the result of a sampling problem inherent in the use of the thin sections that are needed for the electron microscopic classification of the Schwann cell phenotype. It also follows that the absence of X-gal crystals from a particular phenotype does not exclude the possibility of a low level of β-gal expression.

These results confirm and extend previous work, in which immunohistochemistry was used to evaluate the expression of Tst-1/SCIP/Oct-6. Using a relatively insensitive antiserum, Scherer et al. (1994) found Tst-1/SCIP/Oct-6 expression in developing and regenerating rat sciatic nerves but not in adult or in permanently axotomized nerves. With the development of more sensitive antisera, low levels of Tst-1/SCIP/Oct-6 have also been found in Schwann cell precursors, as well as in immature/premyelinating, myelinating, nonmyelinating, and denervated Schwann cells (Blanchard et al., 1996; Zorick et al., 1996). Schwann cells in developing and regenerating nerves have the highest levels of Tst-1/SCIP/Oct-6-immunoreactivity, but the identity of these cells could not be established unequivocally by light microscopy. Our results indicate that these highly Tst-1/SCIP/Oct-6–immunoreactive cells are probably promyelinating Schwann cells. The low level of Tst-1/SCIP/Oct-6 immunoreactivity in Schwann cell precursors, as well as in immature, myelinating, nonmyelinating, and denervated Schwann cells, is consistent with the lower frequency of X-gal and Bluo-gal crystals in bundling, myelinating, nonmyelinating, and denervated Schwann cells. Whether Tst-1/SCIP/Oct-6 plays an important role in these other kinds of Schwann cells is uncertain, because the only phenotype that has been described in *tst-1/scip/oct-6*–null mice is the arrested development at the promyelinating stage (Bermingham et al., 1996; Jaegle et al., 1996).

Transcription factors and the regulation of the Schwann cell phenotype

As shown schematically in Figure 9, several transcription factors are expressed at particular stages of Schwann cell development (Zorick and Lemke, 1996; Scherer, 1997b). Premyelinating, nonmyelinating, and denervated Schwann cells express three unrelated transcription factors, Krox-24, Pax-3, and c-jun (Kioussi et al., 1995; Nikam et al., 1995; Stewart, 1995; Blanchard et al., 1996; Shy et al., 1996). This was shown by *in situ* hybridization for Pax-3 (Kioussi et al., 1995), immunolabeling for c-jun (Shy et al., 1996), and immunolabeling as well as histochemical staining for β-gal in heterozygous knock-out animals for Krox-24 (Nikam et al., 1995; Topilko et al., 1997).

As shown in Figure 9, as Tst-1/SCIP/Oct-6 expression wanes in myelinating Schwann cells, the expression of Krox-20, a zinc

finger transcription factor highly homologous to Krox-24, increases dramatically and remains highly expressed unless Schwann cells become denervated (Topilko et al., 1994, 1997; Murphy et al., 1996; Zorick et al., 1996). Like Tst-1/SCIP/Oct-6, Krox-20 is essential for the normal development of myelinating Schwann cells, because Schwann cells appear to be permanently arrested at the promyelinating stage in *krox-20*–null mice (Topilko et al., 1994).

Although the phenotype of *tst-1*/*scip*/*oct-6*–null mice demonstrates its importance in the development of myelinating Schwann cells, its precise function in this process remains to be determined. In their initial description of Tst-1/SCIP/Oct-6, Monuki et al. (1989) showed that its expression in developing nerves and in forskolin-stimulated Schwann cells precedes that of myelin-related genes. They postulated that Tst-1/SCIP/Oct-6 plays a central role in the differentiation to a myelinating phenotype, but in subsequent transient cotransfection experiments, Tst-1/SCIP/Oct-6 repressed the expression of *mbp* and P_0 promoter constructs in cultured Schwann cells (Monuki et al., 1990, 1993; He et al., 1991). This repression was not observed for other POU family members and depended on both the N terminal and the DNA binding domain of Tst-1/SCIP/Oct-6. However, mutating the Tst-1/SCIP/Oct-6 binding sites in the P_0 promoter did not abolish this repression, leading Monuki et al. (1993) to postulate that Tst-1/SCIP/Oct-6 represses by "squelching," by protein–protein interactions that occur off of DNA. In keeping with the idea that the normal function of Tst-1/SCIP/Oct-6 is to repress the expression of myelin-related genes, transgenic mice expressing an N-terminal–truncated Tst-1/SCIP/Oct-6 driven by a P_0 promoter (ΔTst-1/SCIP/Oct-6) have premature myelination (Weinstein et al., 1995).

The analysis of *tst-1*/*scip*/*oct-6*–null mice, however, does not support the view that the normal function of Tst-1/SCIP/Oct-6 is to repress the expression of myelin-related genes, because the levels of myelin-related mRNAs in neonatal *tst-1*/*scip*/*oct-6*–null mice are normal or reduced (Bermingham et al., 1996; Jaegle et al., 1996). Most myelinating Schwann cells in *tst-1*/*scip*/*oct-6*–null mice are arrested for more than a week at the promyelinating stage; these cells, nevertheless, express and properly localize MAG and periaxin, two myelin-related proteins that are normally expressed by promyelinating Schwann cells. Why the myelin sheaths fails to form at the normal time and, indeed, how the myelinating Schwann cells eventually form them remain unanswered. The identification of the target genes of Tst-1/SCIP/Oct-6 and Krox-20 will prove invaluable in this regard.

REFERENCES

Bermingham Jr JR, Scherer SS, O'Connell S, Arroyo E, Kalla K, Powell FR, Rosenfeld MG (1996) Tst-1/SCIP/Oct-6 regulates a unique step in peripheral myelination and is required for normal respiration. Genes Dev 10:1751–1762.

Blanchard AD, Sinanan A, Parmantier E, Zwart R, Broos L, Meijer D, Meier C, Jessen KR, Mirsky R (1996) Oct-6 (SCIP/Tst-1) is expressed in Schwann cell precursors, embryonic Schwann cells, and postnatal myelinating Schwann cells: comparison with Oct-1, Krox-20, and Pax-3. J Neurosci Res 46:630–640.

Feltri ML, Scherer SS, Wrabetz L, Kamholz J, Shy ME (1992) Mitogen-expanded Schwann cells retain the capacity to myelinate regenerating axons after transplantation into rat sciatic nerve. Proc Natl Acad Sci USA 89:8827–8831.

Gupta SK, Pringle J, Poduslo JF, Mezei C (1993) Induction of myelin genes during peripheral nerve remyelination requires a continuous signal from the ingrowing axon. J Neurosci Res 34:14–23.

Hahn AF, Chang Y, Webster Hd (1987) Development of myelinated nerve fibers in the sixth cranial nerve of the rat: a quantitative electron microscope study. J Comp Neurol 260:491–500.

He X, Gerrero R, Simmons DM, Park RE, Lin CR, Swanson LW, Rosenfeld MG (1991) Tst-1, a member of the POU domain gene family, binds the promoter of the gene encoding the cell surface adhesion molecule P0. Mol Cell Biol 11:1739–1744.

Hollander M, Wolfe DA (1973) The two-sample location problem. In: Nonparametric statistical methods, pp 67–82. New York: Wiley.

Jacobsen KD, Willumsen BM (1995) Kinetics of expression of inducible β-galactosidase in murine fibroblasts: high initial rate compared to steady-state expression. J Mol Biol 252:289–295.

Jaegle M, Mandemakers W, Broos L, Zwart R, Karis A, Visser P, Grosveld F, Meijer D (1996) The POU factor Oct-6 and Schwann cell differentiation. Science 273:507–510.

King RMH, Thomas PK (1971) Electron microscopic observations on aberrant regeneration of unmyelinated axons in the vagus nerve of the rabbit. Acta Neuropathol (Berl) 18:150–159.

Kioussi C, Gross MK, Gruss P (1995) Pax3: a paired domain gene as a regulator in PNS myelination. Neuron 15:553–562.

Kobayashi S, Suzuki K (1990) Development of unmyelinated fibers in peripheral nerve: an immunohistochemical and electron microscopic study. Brain Dev 12:237–246.

Kuhn R, Monuki ES, Lemke G (1991) The gene encoding the transcription factor SCIP has features of an expressed retroposon. Mol Cell Biol 11:4642–4650.

Lee MJ, Brennan A, Blanchard A, Zoidl G, Dong Z, Tabernero A, Zoidl C, Dent MAR, Jessen KR, Mirsky R (1997) P_0 is constitutively expressed in the rat neural crest and embryonic nerves and is negatively and positively regulated by axons to generate non-myelin-forming and myelin-forming Schwann cells, respectively. Mol Cell Neurosci 8:336–350.

Margolis TP, Bloom DC, Dobson AT, Feldman LT, Stevens JG (1993) Decreased reporter gene expression during latent infection with HSV LAT promoter constructs. Virology 197:585–592.

Mirsky R, Jessen KR (1996) Schwann cell development, differentiation and myelination. Curr Opin Neurobiol 6:89–96.

Monuki ES, Weinmaster G, Kuhn R, Lemke G (1989) SCIP: a glial cell POU domain gene regulated by cyclic AMP. Neuron 3:783–793.

Monuki ES, Kuhn R, Weinmaster G, Trapp BD, Lemke G (1990) Expression and activity of the POU transcription factor SCIP. Science 249:1300–1303.

Monuki ES, Kuhn R, Lemke G (1993) Repression of the myelin P0 gene by the POU transcription factor SCIP. Mech Dev 42:15–32.

Morris JH, Hudson AR, Weddell AGM (1972) A study of degeneration and regeneration in the divided rat sciatic nerve base on electron microscopy. IV. Changes in the fascicular microtopography, perineurium and endoneurial fibroblasts. Z Zellforsch Mikrosk Anat 124:165–203.

Murphy P, Topilko P, Schneider-Maunoury S, Seitanidou T, Baron-Van Evercooren A, Charnay P (1996) The regulation of *Krox-20* expression reveals important steps in the control of peripheral glial cell development. Development 122:2847–2857.

Nikam SS, Tennekoon GI, Christy B, Yoshino JE, Rutkowski JL (1995) The zinc finger transcription factor Zif268/Egr-1 is essential for Schwann cell expression of the p75 NGF receptor. Mol Cell Neurosci 6:337–348.

Peters A, Muir AR (1959) The relationship between axons and Schwann cells during development of peripheral nerves in the rat. Q J Exp Physiol 44:117–130.

Scherer SS (1997a) Molecular genetics of demyelination: new wrinkles on an old membrane. Neuron 18:13–16.

Scherer SS (1997b) The biology and pathobiology of Schwann cells. Curr Opin Neurol 10:386–397.

Scherer SS, Easter Jr SS (1984) Degenerative and regenerative changes in the trochlear nerve of goldfish. J Neurocytol 13:519–565.

Scherer SS, Salzer JL (1996) Axon-Schwann cell interactions in peripheral nerve regeneration. In: Glial cell development (Jessen KR, Richardson WD, eds), pp 165–196. Oxford: Bios Scientific.

Scherer SS, Wang D-y, Kuhn R, Lemke G, Wrabetz L, Kamholz J (1994) Axons regulate Schwann cell expression of the POU transcription factor SCIP. J Neurosci 14:1930–1942.

Shy M, Shi Y-j, Wrabetz L, Kamholz J, Scherer SS (1996) Axon-Schwann cell interactions regulate the expression of c-jun in Schwann cells. J Neurosci Res 43:511–525.

Stahl N, Harry J, Popko B (1990) Quantitative analysis of myelin protein

gene expression during development in the rat sciatic nerve. Mol Brain Res 8:209–212.

Stewart HJS (1995) Expression of c-jun, jun B, jun D and cAMP response element binding protein by Schwann cells and their precursors *in vivo* and *in vitro*. Eur J Neurosci 7:1366–1375.

Topilko P, Schneider-Maunoury S, Levi G, Baron-Van Evercooren A, Ben Younes Chennoufi A, Seitanidou T, Babinet C, Charnay P (1994) Krox-20 controls myelination in the peripheral nervous system. Nature 371:796–799.

Topilko P, Murphy P, Charnay P (1996) Embryonic development of Schwann cells: multiple roles for neuregulins along the pathway. Mol Cell Neurosci 8:71–75.

Topilko P, Levi G, Merlo G, Mantero S, Desmarquet C, Mancardi G, Charnay P (1997) Differential regulation of the zinc finger genes *Krox-20* and *Krox-24* (*Egr-1*) suggests antagonistic roles in Schwann cells. J Neurosci Res 50:702–712.

Webster Hd (1993) Development of peripheral nerve fibers. In: Peripheral neuropathy (Dyck PJ, Thomas PK, Low PA, Poduslo JF, eds), pp 243–266. Philadelphia: Saunders.

Weinstein DE, Burrola PG, Lemke G (1995) Premature Schwann cell differentiation and hypermyelination in mice expressing a targeted antagonist of the POU transcription factor SCIP. Mol Cell Neurosci 6:212–229.

Zorick TS, Lemke G (1996) Schwann cell differentiation. Curr Opin Cell Biol 8:870–876.

Zorick TS, Syroid DE, Arroyo E, Scherer SS, Lemke G (1996) The transcription factors SCIP and Krox-20 mark distinct stages and cell fates in Schwann cell differentiation. Mol Cell Neurosci 8:129–145.